

THE CONTRACTILE VACUOLE FLUID DISCHARGE RATE IS DETERMINED BY THE VACUOLE SIZE IMMEDIATELY BEFORE THE START OF DISCHARGE IN *PARAMECIUM MULTIMICRONUCLEATUM*

YUTAKA NAITOH*, TAKASHI TOMINAGA AND RICHARD D. ALLEN

Pacific Biomedical Research Center, Snyder Hall 306, University of Hawaii at Manoa, 2538 The Mall, Honolulu, HI 96822, USA

Accepted 4 April 1997

Summary

The precise relationship between the rate of contractile vacuole fluid discharge and the vacuole diameter at the start of systole was determined in cells of *Paramecium multimicronucleatum* subjected to various external conditions. The rate of discharge was higher when the diameter was larger. When the rate of discharge was plotted against the diameter, the points fell around a single parabolic line passing through the origin and were independent of the external conditions employed. This implies that the rate of discharge is proportional to the square of the vacuole diameter. We have previously

proposed a hypothesis in which membrane tension in the contractile vacuole is altered as its planar membrane becomes tubular or as tubules become planar membrane (termed the membrane area-proportional tension hypothesis). We propose here that it is this change in membrane tension which determines the vacuole pore shape and sets the subsequent rate of fluid discharge.

Key words: *Paramecium multimicronucleatum*, contractile vacuole, fluid discharge rate, vacuole pore size, vacuole membrane tension, vacuole membrane tubulation.

Introduction

It is well known that the contractile vacuole of the freshwater ciliate *Paramecium* changes its size and pulsation frequency to control the fluid output of the cell in response to changes in the external osmotic conditions. The vacuole is larger and the pulsation frequency higher when the external solution is more dilute (Kitching, 1967; Patterson, 1980; Zeuthen, 1992). We recently reported (Naitoh *et al.* 1997) that fluid discharge from contractile vacuoles of *P. multimicronucleatum* *in vivo* was caused by the cytosolic pressure and that the rate of discharge was higher when the vacuole size at the start of discharge (systole) was larger.

According to the Law of Hagen and Poiseuille, the rate of fluid discharge from the contractile vacuole is determined by the pressure difference between the inside of the vacuole and the external solution, and by the width and length of the cylindrical pore of the vacuole. It can be anticipated that the cell will swell more when it is bathed in a dilute solution, as more water will enter the cell under these conditions. The higher rate of discharge from larger vacuoles in dilute solution might, therefore, be attributable to an increased cytosolic pressure due to swelling of the cell. Alternatively, the higher rate of discharge could also be attributable to the change in the pore shape, i.e. widening and/or shortening of the pore. To determine which of these factors, the pressure and/or the pore

shape, affects the rate of fluid discharge, we examined the quantitative relationship between the rate of discharge and the diameter of the vacuole at the start of discharge under various conditions. We conclude that the pore shape of the vacuole, particularly its diameter, is a major factor in determining the rate of fluid discharge from the vacuole. We will also discuss the involvement of tension at the surface membrane of the vacuole, which is proportional to the membrane area (Naitoh *et al.* 1997), in determining the pore shape. Some of the results described in this paper have been presented verbally elsewhere (Allen *et al.* 1996).

Materials and methods

Cells of *P. multimicronucleatum* (syngen 2) (Allen *et al.* 1988) were grown in an axenic culture medium (Fok and Allen, 1979) and were harvested at the mid-logarithmic growth phase. These cells were washed with a standard saline solution containing (final concentration in mmol l^{-1}): 0.5 NaCl, 2.0 CaCl_2 , 1.0 MgCl_2 , 1.0 KCl and 1.0 Tris-HCl buffer (pH 7.4). Cells were then transferred into each experimental solution and equilibrated for more than 40 min prior to experimentation. The solutions employed were a standard saline solution, a saline solution diluted with water to 1/10 or 1/100 of the

*e-mail:naitoh@pbrc.hawaii.edu.

original concentration and an 80 mmol l^{-1} sorbitol-containing saline solution.

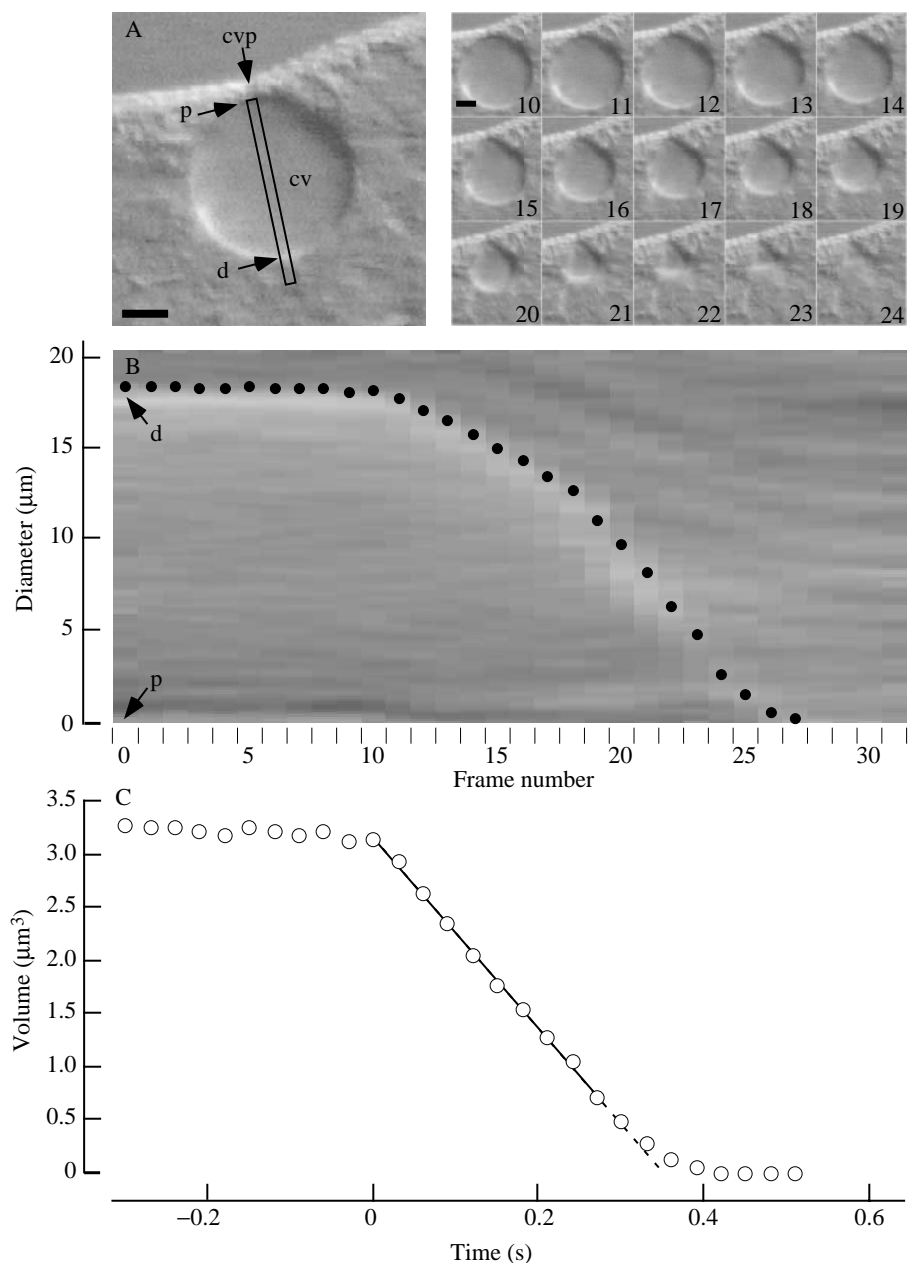
Equilibrated cells were slightly compressed between a glass slide and a coverslip by introducing $20 \mu\text{m}$ diameter polystyrene beads into the medium. Profile views of contractile vacuoles were video-recorded (AG-6300, Panasonic Indust. Co., Secaucus, NJ, USA) at 30 ms per frame using Nomarski microscope optics (Leitz $\times 60$ objective, Leica Mikrosk. u. System, GmbH, Wetzlar, Germany) and a video camera (CCD-72, Dage MIT Inc., Michigan City, IN, USA). Video images were fed into a computer (Power Macintosh 7100/80, Apple Computer Inc., Cupertino, CA, USA) using a frame grabber (LG-3, Scion Corp., Frederick, MD, USA) for analysis of the time course of the change in vacuole diameter during systole (Inoué, 1986). The analysis was performed using the public

domain NIH Image Program (developed at the US National Institutes of Health and available on the Internet at <http://rsb.info.nih.gov/nih-image/>).

As shown in Fig. 1, the contractile vacuole was essentially spherical in the early and middle stages of systole. Later, it took on the shape of an 'Erlenmeyer flask' as a result of the presence of microtubules extending from the pore region and passing over the region of the vacuole next to the pore (Hausmann and Allen, 1977). For this reason, we measured the vacuole diameter only in the early and middle phases of systole to determine the rate of discharge.

For electron microscopy, a cell in a small droplet of saline solution was fixed instantaneously by squirting a fixative containing 2% glutaraldehyde in 0.05 mol l^{-1} cacodylate buffer against the cell through a fine-bore pipette placed close to the

Fig. 1. A computer-aided display of a contractile vacuole in profile view obtained from a cell of *Paramecium multimicronucleatum* together with graphs for determining the rate of fluid discharge from a vacuole. (A) Right, consecutive images of a discharging vacuole displayed every 30 ms. The number on each image is the frame number corresponding to that in B. Scale bar, $5 \mu\text{m}$. (A) Left, an enlarged image of the contractile vacuole at frame number 10. A slit-like area on the image marked by a long rectangle corresponds to the diameter of the vacuole. cv, contractile vacuole; cvp, contractile vacuole pore; p, the end of the diameter proximal to the pore; d, the end of the diameter distal from the pore. Scale bar, $5 \mu\text{m}$. (B) Time course of the change in vacuole diameter during systole. The slit-like image corresponding to vacuole diameter, as obtained from each consecutive vacuole image in A (right), is displayed in accordance with the frame number, so that images corresponding to d give the time course of change in the vacuole diameter. Filled circles, values for the diameters of the images of the vacuole in A (right). (C) Time course of the change in the volume of the vacuole during systole. Open circles, the volume of the vacuole calculated from the corresponding values for the diameter of the vacuole shown in B. The straight line is a linear regression line fitted to 10 circles corresponding to the volume of the vacuole at times corresponding to frame numbers 10–19 ($r^2=0.9986$). The slope of this line corresponds to the rate of vacuole fluid discharge.



cell. The precise moment of fixation was monitored through a video camera, and the phase of discharge was later determined by observing the resulting video frames. Conventional techniques (Allen and Fok, 1988) were employed for obtaining the subsequent electron micrographs of the same cells as recorded by video microscopy. All the experiments were performed at a room temperature of 24–26 °C.

Results

The internal diameters of contractile vacuoles at the start of systole (their initial diameters) and their rates of fluid discharge were determined in three groups of cells treated with three different solutions; standard saline solution, 1/10-diluted saline solution and 80 mmol l⁻¹ sorbitol-containing saline solution. As shown in Fig. 2, the rate of discharge was significantly higher in 1/10-diluted saline solution and lower in 80 mmol l⁻¹ sorbitol-containing saline solution than in standard saline solution (ANOVA, $P < 0.01$). The initial diameters were significantly larger in 1/10-diluted saline solution and smaller in 80 mmol l⁻¹ sorbitol-containing saline solution than in standard saline solution (ANOVA, $P < 0.01$). It is clear that the rate of discharge was higher in the cell

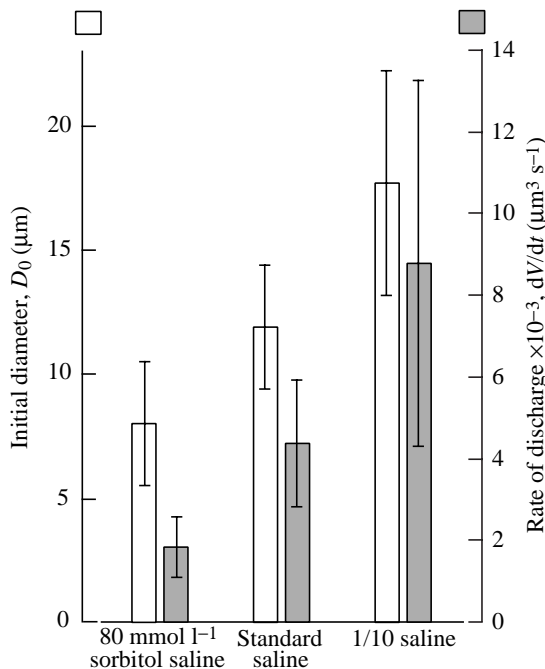


Fig. 2. The initial diameters of contractile vacuoles at the start of systole (open columns) and their rates of fluid discharge (shaded bars) from three groups of cells of *Paramecium multimicronucleatum* equilibrated in three different solutions. In standard saline solution, the mean diameter and rate of discharge were $11.9 \pm 2.5 \mu\text{m}$ and $4.4 \times 10^3 \pm 1.5 \times 10^3 \mu\text{m}^3 \text{s}^{-1}$ ($N=34$), respectively. In 1/10-diluted saline solution, the mean diameter and rate of discharge were $17.7 \pm 4.5 \mu\text{m}$ and $8.8 \times 10^3 \pm 4.5 \times 10^3 \mu\text{m}^3 \text{s}^{-1}$ ($N=56$), respectively. In 80 mmol l⁻¹ sorbitol-containing saline solution, the mean diameter and rate of discharge were $8.0 \pm 1.3 \mu\text{m}$ and $1.8 \times 10^3 \pm 0.7 \times 10^3 \mu\text{m}^3 \text{s}^{-1}$ ($N=33$), respectively. The vertical bar in each column is the standard deviation.

group where the contractile vacuoles had larger initial diameters.

To examine the relationship between the rate of discharge and the initial vacuole diameter, the values for the rates of discharge for all contractile vacuoles obtained from the three different groups of cells treated with three different solutions, i.e. standard saline solution, 1/10-diluted saline solution and 80 mmol l⁻¹ sorbitol-containing solution, were plotted against their respective initial diameters (Fig. 3). All the points in the figure were distributed close to the same curved line.

During the course of these experiments, we also found that the initial vacuole diameter at which the vacuole enters systole changed after a cell had been compressed in a thin (20 μm) space. The time course for the change in the initial diameter and that for the rate of discharge after compression were determined in the same cell bathed in standard saline solution. A representative result is shown in Fig. 4. The initial diameter (open circles in Fig. 4), 13.5 μm at the beginning of compression, decreased to a minimum value of 11.3 μm approximately 6 min after the start of compression. The diameter then gradually increased to an approximately steady value of 12.2 μm at 40 min after the start of compression. The rate of discharge (triangles in Fig. 4) changed in parallel with the change in the initial diameter, i.e. the rate was $5.3 \times 10^3 \mu\text{m}^3 \text{s}^{-1}$ at the beginning of compression and decreased

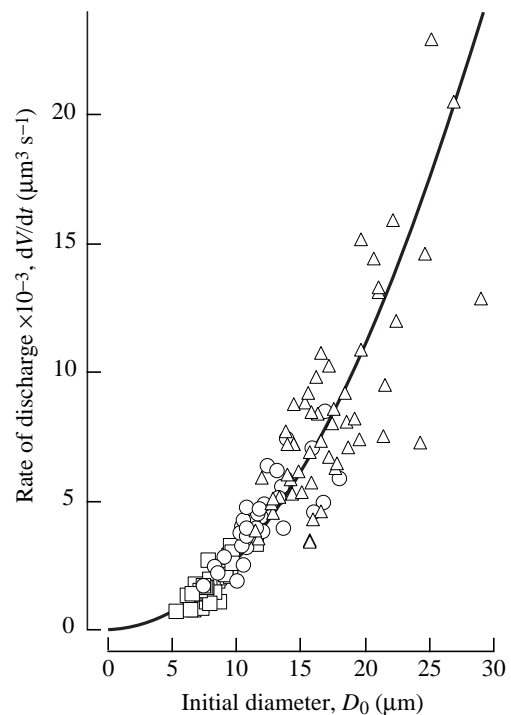


Fig. 3. The relationship between the rate of fluid discharge (dV/dr) and the diameter of the contractile vacuole at the start of systole (initial diameter D_0) from three groups of cells of *Paramecium multimicronucleatum* equilibrated in three different solutions. Circles, in standard saline solution. Triangles, in 1/10-diluted saline solution. Squares, in 80 mmol l⁻¹ sorbitol-containing saline solution. The curved line corresponds to equation 2 in the text.

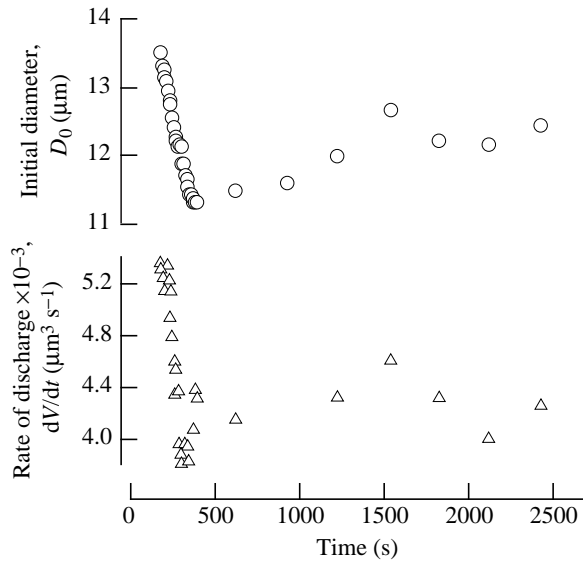


Fig. 4. (A) A representative plot of changes in the initial diameter (open circles) and the rate of discharge (triangles) of a single contractile vacuole after compression of a *Paramecium multimicronucleatum* cell. The cell was equilibrated in standard saline solution and compressed between a coverslip and a glass slide (approximately 20 μm).

to a minimum value of $3.8 \times 10^3 \mu\text{m}^3 \text{s}^{-1}$ approximately 6 min after the start of compression. The rate then increased to a steady value of approximately $4.3 \times 10^3 \mu\text{m}^3 \text{s}^{-1}$ at 40 min after the start of compression.

To determine whether the vacuole pore morphology changes with an increase or decrease in the discharge rate, the cells were first treated with four different solutions (standard saline solution, 1/10-diluted saline solution, 1/100-diluted saline solution and 80 mmol l^{-1} sorbitol-containing saline solution) in order to obtain

cells with contractile vacuoles that had different initial diameters. The cells were then individually fixed at a specific phase of the contractile vacuole cycle. Each vacuole was then serially sectioned, and electron micrographs were used to determine the diameter and the length (depth) of the pore. Fig. 5A shows a representative micrograph of a contractile vacuole in late systole obtained from a cell treated with standard saline solution, and Fig. 5B shows a micrograph of 40 nm membrane tubules that are bound to the bands of microtubule ribbons that arise from the vacuole pore. Table 1 shows morphological data obtained for 15 contractile vacuole pores obtained from 10 different cells. The mean value for the pore diameter was $1.5 \pm 0.3 \mu\text{m}$ ($N=15$) and for the pore length was $2.0 \pm 0.2 \mu\text{m}$ ($N=9$; mean \pm S.D.).

Discussion

Is the cytosolic pressure or the vacuole pore size responsible for the change in the rate of fluid discharge?

An approximate cytosolic pressure when the cells were in standard saline solution was calculated according to the Law of Hagen and Poiseuille using a vacuole discharge rate of $4.4 \times 10^3 \mu\text{m}^3 \text{s}^{-1}$ (Fig. 2), a vacuole pore radius of 0.75 μm and a vacuole pore length of 2.0 μm (Table 1) to be 73 N m^{-2} . This pressure is far smaller than the osmotic pressure difference (approximately $5 \times 10^5 \text{ N m}^{-2}$) would be between a standard saline solution (approximately 15 mosmol l^{-1}) and the cytosol (approximately 200 mosmol l^{-1}). However, this pressure is larger than the cytosolic pressure of some marine invertebrate eggs (approximately 5 N m^{-2}) (Cole, 1932; Yoneda, 1964). In marine invertebrate eggs, the osmotic pressure difference between sea water and the cytosol is negligible and, therefore, the cytosolic pressure is caused solely by tension at the cell surface (surface boundary tension and/or membrane elastic tension) (Harvey, 1954). In contrast, cells of *P.*

Table 1. Contractile vacuole pore of *Paramecium multimicronucleatum* examined on electron micrographs and video images

Cell number	Treatment	Anterior vacuole				Posterior vacuole			
		Initial diameter, D_0 (μm)	Pore diameter, $2R$ (μm)	Pore length, L (μm)	Pulsation phase	Initial diameter, D_0 (μm)	Pore diameter, $2R$ (μm)	Pore length, L (μm)	Pulsation phase
1	std	7.8	1.0	1.6	D	8.5	1.3	—	RO
2	std	10.4	1.7	2.2	LS	—	1.3	—	—
3	std	—	1.5	2.0	—	—	1.8	1.7	—
4	1/10	13.5	1.8	—	LS	—	—	—	—
5	1/10	18.0	1.3	—	RO	14.6	1.5	—	D
6	1/10	—	—	—	—	9.5	1.8	2.0	RO
7	1/10	15.6	2.3	2.1	MS	—	—	—	—
8	1/100	12.8	1.4	—	LS	—	—	—	—
9	80	8.3	1.4	2.2	RO	7.3	1.4	2.3	D
10	80	—	—	—	—	—	1.7	2.1	—

Cells were treated with standard saline solution (std); with 1/10-diluted saline solution (1/10), with 1/100-diluted saline solution (1/100) and with 80 mmol l^{-1} sorbitol-containing saline solution (80).

Pulsation phase: cells were fixed when the vacuole was at the diastolic phase (D), at the rounded stage immediately before the start of systole (RO), at the early systolic phase (ES), at the mid-systolic phase (MS) and at the late systolic phase (LS). Pulsation phases and D_0 were estimated from video images of each contractile vacuole (see Materials and methods for details).

R is the pore radius; bars, measurements could not be made.

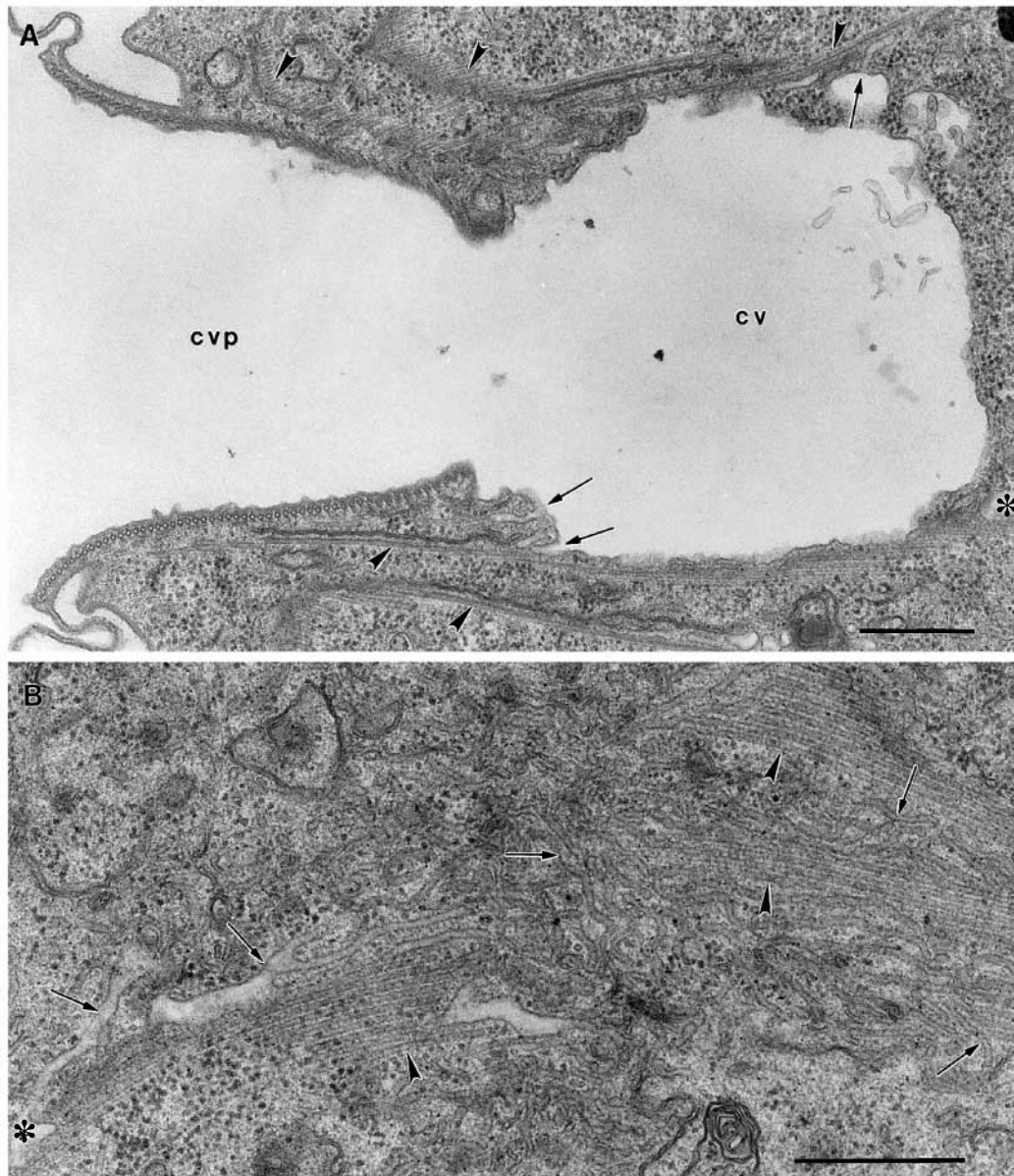


Fig. 5. Two electron micrographs from adjacent regions of the same contractile vacuole in late systole in a *Paramecium multimicronucleatum* cell equilibrated in standard saline solution. (A) This contractile vacuole pore is approximately funnel-shaped rather than cylindrical and the vacuole is nearly collapsed. Contractile vacuole membrane is associated with cytoskeletal microtubular ribbons (arrowheads). Signs of ongoing tubulation of the more planar vacuole membrane can be detected near the ribbons (arrows) (asterisks in A and B indicate where A and B overlap). (B) Microtubules form ribbons of regularly spaced elements (arrowheads), while the bulk of the contractile vacuole membrane forms 40 nm membrane tubules that are branched and are irregularly oriented with respect to neighbouring membranous tubules (arrows). Tubules are found only on the side of the ribbons bordering the space previously occupied by the contractile vacuole. cvp, contractile vacuole pore; cv, contractile vacuole. Scale bars, 0.5 μm .

multimicronucleatum are hyperosmotic to their environment (approximately $200 \text{ mosmol l}^{-1}$ for the cytosol versus 40 mosmol l^{-1} for the culture medium). The external water, therefore, enters the cell continuously through the water-permeable cell membrane, and much of the excess water must be expelled through the contractile vacuole system (Patterson, 1980). The cytoplasm of *P. multimicronucleatum*, therefore, must exert a slight positive pressure on the cell membrane, together with its associated cytoskeletal elements, due to the

swelling of the cell that offsets the osmotic pressure. Linder and Staehelin (1979) estimated the pressure difference between the lumen of the contractile vacuole and the external solution (in the flagellar pocket) in the flagellate *Leptomonas collosoma*, on the basis of the rate of fluid discharge and the pore size, to be $6.7 \times 10^4 \text{ N m}^{-2}$. This value is higher than the value calculated for *P. multimicronucleatum*.

The rate of fluid output through the contractile vacuole system of *Paramecium* is higher when the cell is in more dilute

solution (Ishida *et al.* 1993; Kitching, 1967; Patterson, 1980; Zeuthen, 1992). It is, therefore, highly probable that the degree of osmotic swelling of the cell that determines the cytosolic pressure is kept approximately constant irrespective of changes in the external osmotic pressure, at least in the range we have employed (see also Rifkin, 1973, for *Tetrahymena pyriformis*).

However, we initially assumed that compression of the cell should increase the cytosolic pressure. Therefore, it seemed reasonable to predict that the rate of discharge of a vacuole would be increased by cellular compression. Contrary to this prediction, however, the rate of discharge of a vacuole decreased after compression (Fig. 4). Previously we had found (Naitoh *et al.* 1997) that disruption of the decorated spongione, the locus of fluid segregation in *P. multimicronucleatum* (Ishida *et al.* 1993), did not change the rate of discharge from a filled vacuole, although the cell tended to swell due to the overall decrease in fluid output. These findings suggest that osmotic swelling of a cell or a mechanical compression of the cell, at least to the extent used in the present experiments, does not produce an increase in the cytosolic pressure large enough to bring about a significant increase in the rate of contractile vacuole discharge. In other words, the cytosolic pressure remains almost constant under the experimental conditions employed. The change in the pore shape may therefore be responsible for the change in the fluid discharge rate when the cells are subjected to different external conditions, although the exact cause remains to be determined.

Is the pore length or the pore width responsible for the change in the rate of fluid discharge?

According to the Law of Hagen and Poiseuille, the rate of fluid discharge from a cylindrical vacuole pore, can be written as:

$$\frac{dV}{dt} = \frac{\pi R^4}{8\eta L} P, \quad (1)$$

where V is the volume of the vacuole, t is the time, R is the radius of the vacuole pore, L is the length (depth) of the vacuole pore, P is the cytosolic pressure and η is the viscosity of the fluid (constant). As discussed in the previous section, P was assumed to be constant under the experimental conditions employed. The rate of discharge is, therefore, proportional to R^4/L .

The rate of discharge was $8.8 \times 10^3 \pm 4.5 \times 10^3 \mu\text{m}^3 \text{s}^{-1}$ ($N=56$) from vacuoles in cells equilibrated in 1/10-diluted saline solution. This value is approximately five times larger than that for the rate from vacuoles in cells equilibrated in 80 mmol l^{-1} sorbitol-containing saline solution ($1.8 \times 10^3 \pm 0.7 \times 10^3 \mu\text{m}^3 \text{s}^{-1}$, $N=33$) (Fig. 2). If R were to remain unchanged during the switch from a dilute to a more concentrated solution, then L in 80 mmol l^{-1} sorbitol-containing saline solution would be five times longer than that in 1/10-diluted saline solution. Conversely, if L were to remain unchanged, then R in 1/10-diluted saline solution would be 1.5 times wider than that in 80 mmol l^{-1} sorbitol-containing saline solution.

Our examination of serial-sectioned vacuole pores by electron microscopy (Table 1) showed no obvious differences in L and R between those vacuoles in 1/10-diluted saline solution (L , $2.1 \mu\text{m}$; R , $0.87 \mu\text{m}$) and those in 80 mmol l^{-1} sorbitol-containing saline solution (L , $2.2 \mu\text{m}$; R , $0.75 \mu\text{m}$), although the sample size was too small to examine the measured values statistically. It is apparent that the shape of the vacuole can be somewhat distorted when the vacuole is subjected to electron microscopical procedures. It is, therefore, conceivable that a 1.5-fold increase in R in the 1/10-diluted saline solution would not be easily recognizable in the electron micrographs. In contrast, a fivefold increase in L should be detectable even though the shape of the vacuole becomes fairly distorted after fixation and sectioning for electron microscopy. Since we never saw such a large elongation of the vacuole pore, we concluded that a change in the pore radius is the major cause for the change in the rate of discharge. This, however, does not rule out some minor change in the pore length. It can be concluded that the vacuole pore is wider (and somewhat shorter) when the overall vacuole size is larger at the beginning of systole. In this connection, it should be noted that a widening and a shortening of the contractile vacuole pore were reported during the diastolic phase of vacuole filling in *T. pyriformis*. This was demonstrated electron microscopically many years ago by Cameron and Burton (1969).

Is the diameter, the membrane area or the volume of the vacuole most closely correlated with its rate of discharge?

To determine the relationship between vacuole size at the start of systole and vacuole pore size, as represented by the rate of discharge, all the data presented in Figs 3 and 4 were combined and replotted on a logarithmic scale (Fig. 6). A straight line with the slope of 2 was drawn according to the least-squares method so as to fit all the points in the figure ($\chi^2=1.777$, $N=156$). It is clear from this figure that the different groups of cells, irrespective of treatment, were all distributed along this line. The slope of 2 implies that the membrane area is proportional to the rate of discharge. This suggests that the vacuole membrane area affects the vacuole pore shape in the same way when the external conditions are changed.

The line could be formulated as:

$$\frac{dV}{dt} = 28.2(\pm 0.7)D_0^2, \quad (2)$$

where D_0 is the diameter of the vacuole at the start of systole. The parabolic line in Fig. 3 corresponds to equation 2.

How does the membrane area affect the vacuole pore shape?

In our previous paper (Naitoh *et al.* 1997), we proposed a hypothesis that the internal pressure of a contractile vacuole in a ruptured cell is caused by the tension of the vacuole membrane. The tension would be proportional to the planar vacuole membrane area. This tension would be generated as the 40 nm (diameter) tubules became flattened into an essentially planar vacuole membrane. Membrane tubulation

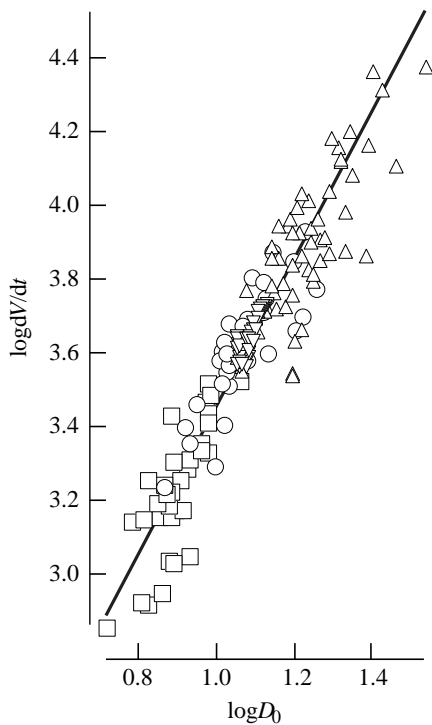


Fig. 6. The relationship between the rate of fluid discharge from the contractile vacuole (dV/dt) and the initial diameter of the vacuole (D_0) for four groups of cells of *Paramecium multimicronucleatum* subjected to four different external conditions. All the data included in Figs 3 and 4 have been plotted on a logarithmic scale. Circles, cells equilibrated in standard saline solution. Triangles, cells equilibrated in 1/10-diluted saline solution. Squares, cells equilibrated in 80 mmol l^{-1} sorbitol-containing saline solution. Inverted triangles, a cell compressed between a glass slide and a coverslip ($20 \mu\text{m}$) in standard saline solution. The straight line is a line with a slope of 2 drawn according to the least-squares method to give the best fit to all the points in the figure.

had previously been reported to occur when the vacuoles of normal (unruptured) cells entered systole (Allen and Fok, 1988). It is, therefore, conceivable that membrane tubulation-related tension is responsible for determining the pore shape.

The contractile vacuole membrane is anchored to the microtubule ribbons which originate from around the vacuole pore (Fig. 5) (Hausmann and Allen, 1977). Stretching of the pore structure caused by a build-up of membrane tension as more tubules become flattened to form the expanding contractile vacuole could conceivably bring about a shortening and/or a widening of the pore.

The presence of a ratchet mechanism to keep the vacuole pore size fixed

As shown in Fig. 1C, the rate of fluid discharge was constant during the early and middle phases of systole (Naitoh *et al.* 1997). This suggests the presence of a ratchet mechanism in the pore structure which keeps the pore shape constant during systole. Thus, the shape of the pore is set by the membrane tension immediately before the start of each

discharge. It should also be noted that the rate of vacuole discharge, in the last stage of systole, varies from this earlier constant rate. This is clearly shown in Fig. 1C, where values deviated upwards from the straight line at all points in the late phase of systole. It is clear that the rate of discharge decreases in the late phase of systole, suggesting that the vacuole pore size decreases, most probably as a result of narrowing of the vacuole pore.

At present, we do not know what cytoskeletal structure corresponds to this hypothetical ratchet mechanism or how this structure could function as a ratchet. However, it is highly probable that the mechanism resides in the helically arranged microtubules surrounding the pore membrane (Hausmann and Allen, 1977; McKanna, 1973). As early as 1967, McIntosh and Porter proposed a hypothetical mechanism for generating a force capable of bringing about a sustained constriction of the sperm head by a highly ordered helical array of microtubules.

Some other considerations

According to biophysical studies on the fusion of phospholipid bilayers and vesicles (Chernomordik *et al.* 1995), an increase in bilayer tension was a key factor for promoting fusion. In their patch-clamp studies on the degranulation of mast cells, Monck and Fernandez (1992) and Monck *et al.* (1990) found that high membrane tension in the secretory granule was the critical stress for bringing about its exocytotic fusion. It is, therefore, probable that stretching of membrane tubules to cause tension is involved in the contractile vacuole pore opening, in which fusion of the vesicle membrane with the plasma membrane covering the pore occurs at the start of each systole.

This work was supported by NSF Grant MCB 95 05910.

References

- ALLEN, R. D. AND FOK, A. K. (1988). Membrane dynamics of the contractile vacuole complex of *Paramecium*. *J. Protozool.* **35**, 63–71.
- ALLEN, R. D., TOMINAGA, T. AND NAITOH, Y. (1996). Spontaneous membrane tubulation can produce sufficient work to account for *in vivo* contractile vacuole expulsion. *Molec. Biol. Cell* **7**, 449.
- ALLEN, R. D., UENO, M. S. AND FOK, A. K. (1988). A survey of lectin binding in *Paramecium*. *J. Protozool.* **35**, 400–407.
- CAMERON, I. L. AND BURTON, A. L. (1969). On the cycle of the water expulsion vesicle in the ciliate *Tetrahymena pyriformis*. *Trans. Am. microsc. Soc.* **88**, 386–393.
- CHEMNOMORDIK, L., KOZLOV, M. M. AND ZIMMERBERG, J. (1995). Lipids in biological membrane fusion. *Membr. Biol.* **146**, 1–14.
- COLE, K. S. (1932). Surface force of the *Arbacia* egg. *J. cell. comp. Physiol.* **1**, 1–9.
- FOK, A. K. AND ALLEN, R. D. (1979). Axenic *Paramecium caudatum*. I. Mass culture and structure. *J. Protozool.* **26**, 463–470.
- HARVEY, E. N. (1954). The tension at the cell surface. In *Protoplasmotologia*, vol. II (ed. L. V. Heilbrunn and F. Weber), E5, pp. 1–30. Wein: Springer Verlag.
- HAUSMANN, K. AND ALLEN, R. D. (1977). Membranes and

- microtubules of the excretory apparatus of *Paramecium caudatum*. *Eur. J. Cell Biol.* **15**, 303–320.
- INOUE, S. (1986). *Video Microscopy*. New York, London: Plenum Press.
- ISHIDA, M., AIHARA, M. S., ALLEN, R. D. AND FOK, A. K. (1993). Osmoregulation in *Paramecium*: the locus of fluid segregation in contractile vacuole complex. *J. Cell Sci.* **106**, 693–702.
- KITCHING, J. A. (1967). Contractile vacuoles, ionic regulation and excretion. In *Research in Protozoology*, vol. 1 (ed. T. T. Chen), pp. 307–336. London: Pergamon Press.
- LINDER, J. C. AND STAEHELIN, A. (1979). A novel model for fluid secretion by the trypanosomatid contractile vacuole apparatus. *J. Cell Biol.* **83**, 371–382.
- MCINTOSH, J. R. AND PORTER, K. R. (1967). Microtubule in the spermatids of the domestic fowl. *J. Cell Biol.* **35**, 153–173.
- MCKANNA, J. A. (1973). Fine structure of the contractile vacuole pore in *Paramecium*. *J. Protozool.* **20**, 631–638.
- MONCK, J. R., ALVAREZ-DE-TOLEDO, G. AND FERNANDEZ, J. M. (1990). Tension in secretory granule membranes causes extensive membrane transfer through the exocytotic fusion pore. *Proc. natn. Acad. Sci. U.S.A.* **87**, 7804–7808.
- MONCK, J. R. AND FERNANDEZ, J. M. (1992). The exocytotic fusion pore. *J. Cell Biol.* **119**, 1395–1404.
- NAITOH, Y., TOMINAGA, T., ISHIDA, M., FOK, A. K., AIHARA, M. S. AND ALLEN, R. D. (1997). How does the contractile vacuole of *Paramecium multimicronucleatum* expel fluid? Modelling the expulsion mechanism. *J. exp. Biol.* **200**, 713–721.
- PATTERSON, D. J. (1980). Contractile vacuole and associated structures: Their organization and function. *Biol. Rev.* **55**, 1–46.
- RIFKIN, J. L. (1973). The role of the contractile vacuole in the osmoregulation of *Tetrahymena pyriformis*. *J. Protozool.* **20**, 108–114.
- YONEDA, M. (1964). Tension at the surface of sea-urchin eggs. A critical examination of Cole's experiment. *J. exp. Biol.* **41**, 893–906.
- ZEUTHEN, T. (1992). From contractile vacuole to leaky epithelia. Coupling between salt and water fluxes in biological membranes. *Biochim. biophys. Acta* **1113**, 229–258.